DOI:10.1021/jf101417w

JOURNAL OF AGRICULTURAL AND FOOD CHEMISTRY
ARTICLE

Binding of Oxytetracycline to Bovine Serum Albumin: Spectroscopic and Molecular Modeling Investigations

Zhenxing Chi, Rutao Liu,* Yue Teng, Xiaoyan Fang, and Canzhu Gao

School of Environmental Science and Engineering, Shandong University, China−America CRC for Environment and Health, Shandong Province, 27# Shanda South Road, Jinan 250100, People's Republic of China

The residue of the widely used veterinary drug oxytetracycline (OTC) in the environment (e.g., animal food, soils, surface water, and groundwater) is potentially harmful. Knowledge of its binding to proteins contributes to the understanding of its toxicity in vivo. This work establishes the binding mode of OTC with bovine serum albumin (BSA) under physiological conditions by spectroscopic methods and molecular modeling techniques. The inner filter effect was eliminated to get accurate data (binding parameters). On the basis of the thermodynamic results and site marker competition experiments, it was considered that OTC binds to site II (subdomain IIIA) of BSA mainly by electrostatic interaction. Furthermore, using the BSA model established with CPHmodels, molecular docking and some other molecular modeling methods were applied to further define that OTC interacts with the Arg 433, Arg 436, Ala 429, and Pro 516 residues of BSA. In addition, UV−visible absorption, synchronous fluorescence, and circular dichroism (CD) results showed that the binding of OTC can cause conformational and some microenvironmental changes of BSA. The work provides accurate and full basic data for clarifying the binding mechanisms of OTC with BSA in vivo and is helpful for understanding its effect on protein function during its transportation and distribution in blood.

KEYWORDS: Oxytetracycline; bovine serum albumin; multispectroscopic techniques; molecular modeling; noncovalent binding; inner filter effect

INTRODUCTION

Serum albumin is the most abundant protein (*1*) in the circulatory system of a wide variety of vertebrates (accounting for 52−60% of the total plasma protein) (*2*, *3*). The most important physiological functions of serum albumin are to maintain the osmotic pressure and pH of blood and to transport a wide variety of endogenous and exogenous compounds (*1*), including drugs and nutrients, mostly through the formation of noncovalent complexes at specific binding sites (*3*). The absorption, distribution, metabolism, and excretion properties as well as the stability and toxicity of drugs can be significantly affected as a result of their binding to serum albumins (*4*). Moreover, there is evidence of conformational changes of serum albumin induced by its interaction with low molecular weight drugs, which may affect serum albumin's biological function as the carrier protein (*1*, *4*). Consequently, investigation of the interaction of drugs including veterinary drugs to serum albumin is of great importance. As a kind of serum albumin, bovine serum albumin (BSA) has the advantages of medical importance, low cost, ready availability, and unusual ligand-binding properties. Bovine and human serum albumin tertiary structures are 76% similar, and the results of all studies are consistent with the fact that human and bovine serum albumin are homologous proteins (*5*).

*Author to whom correspondence should be addressed (phone/fax 86-531-88364868; e-mail rutaoliu@sdu.edu.cn).

Oxytetracycline (OTC), the structure of which is shown in the inset of **Figure 1**, is widely used for the therapy of infectious diseases of animals in intensive farming systems and aquaculture due to its broad-spectrum antibiotic activity (*6*−*9*). Because of its low bioavailability (*10*), only a fraction of the ingested OTC is metabolized in the animals, and the residual OTC is excreted and released into soils, surface water, and groundwater, bringing significant environmental problems (*10*, *11*). The effect of OTC contamination on human health has aroused worldwide attention and research on the toxicity of OTC at the whole organism level (*10*−*12*), organ level (*13*), and cellular level (*14*). The interaction between OTC and serum albumin at the molecular level by using spectroscopic methods (*15*−*18*) has also been studied, but the inner filter effect was not considered. For the BSA−OTC system, the inner filter effect is caused by the absorption of the excitation and emission wavelengths by OTC and BSA in fluorescence experiments, which change the intensity of fluorescence spectra of BSA, affecting the binding parameters calculated from the fluorescence data. In addition, the binding sites of OTC to BSA have not previously been identified. These two aspects hinder our proper and comprehensive understanding of the interaction between the veterinary drug OTC and BSA in vivo.

In the present work, we simulated the interaction between OTC and BSA during blood transportation process in vitro under physiological conditions by spectroscopic and molecular modeling methods. The inner filter effect was corrected before we

 Published on Web 08/27/2010

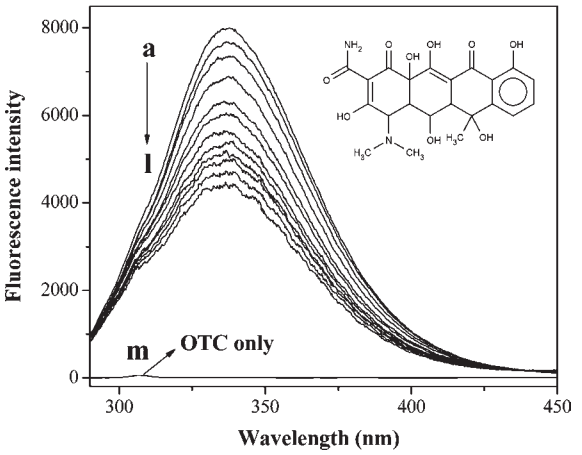

Figure 1. Effect of OTC on BSA fluorescence (corrected). Conditions: BSA, 1.0×10^{-6} mol L^{-1}; OTC/(10^{-5} mol L^{-1}), a, 0; b, 0.2; c, 0.4; d, 0.8; e, 1.2; f, 1.6; g, 2; h, 2.4; i, 2.8; j, 3.2; k, 3.6; l, 4; m, OTC only, 4×10^{-5} mol L^{-1}; pH 7.4; T = 301 K.

estimated the association constants, thermodynamic parameters, number of binding sites, binding forces, and energy transfer distance of the interaction between OTC and BSA. The specific binding site of OTC on BSA was investigated. The effect of OTC on the microenvironment and conformation of BSA was also discussed. The study provides accurate and full basic data for clarifying the binding mechanisms of OTC with serum albumin in vivo and is helpful for understanding its effect on protein function during the blood transportation process and its toxicity in vivo.

MATERIALS AND METHODS

Reagents. BSA (Sinopharm Chemical Reagent Co., Ltd.) was dissolved in ultrapure water to form a 1.0×10^{-5} mol L^{-1} solution and then stored at 0−4 °C and diluted as required. A stock solution of OTC (1.0×10^{-3} mol L^{-1}) was prepared by dissolving 0.0461 g of OTC (Beijing Shanglifang Joint Chemical Technology Research Institute) in 100 mL of water. Hydrochloric acid solution (1:1, 0.5 mL) was used to promote dissolution. Phenylbutazone (PB), flufenamic acid (FA), and digitoxin (TCI-GR, Tokyo Chemical Industry Co., Ltd., Japan) were dissolved in ethanol to form a 1.0×10^{-3} mol L^{-1} solution, which was used to determine the binding sites of OTC at BSA. A 0.2 mol L^{-1} mixture of phosphate buffer (mixture of $NaH_2PO_4 \cdot 2H_2O$ and $Na_2HPO_4 \cdot 12H_2O$, pH 7.4) was used to control the pH. Ultrapure water was used throughout the experiments.

Fluorescence Measurements. All fluorescence spectra were recorded on an F-4600 spectrofluorometer (Hitachi, Japan). To each of a series of 10 mL test tubes were successively added 1.0 mL of 0.2 mol L^{-1} phosphate buffer (pH 7.4), 1.0 mL of 1.0×10^{-5} mol L^{-1} BSA, and different amounts of 1.00×10^{-3} mol/L stock solution of OTC. After equilibration for 20 min, the fluorescence spectra were then measured (excitation wavelength at 278 nm and emission wavelengths of 290−450 nm). The excitation and emission slit widths were set at 5.0 nm. The scan speed was 1200 nm/min. Photo multiplier tube (PMT) voltage was 700 V. The synchronous fluorescence spectra were measured at λ_{ex} = 250 nm, $\Delta\lambda$ = 15 nm, and $\Delta\lambda$ = 60 nm.

UV−Visible Absorption Measurements. The absorption spectra were recorded on a UV-2450 spectrophotometer (Shimadzu, Kyoto, Japan) equipped with 10 mm quartz cells. Slit width was set at 2.0 nm. The wavelength range was 200−450 nm.

Circular Dichroism (CD) Measurements. CD spectra were collected from 200 to 260 at 0.2 nm intervals on a JASCO J-810 CD spectrometer using a quartz cell with a path length of 10 mm. The scanning speed was set at 200 nm/min. Three scans were made and averaged for each CD spectrum.

Molecular Modeling Study. Docking calculations were carried out using Docking Server. The MMFF94 force field (*19*) was used for energy minimization of the ligand molecule (OTC) using Docking Server. Gasteiger partial charges were added to the ligand atoms. Nonpolar hydrogen atoms were merged, and rotatable bonds were defined.

Docking calculations were carried out on a BSA protein model, which was modeled with CPHmodels (*20*). Essential hydrogen atoms, Kollman united atom type charges, and solvation parameters were added with the aid of AutoDock tools (*21*). Affinity (grid) maps of 20 × 20 × 20 Å grid points and 0.375 Å spacing were generated using the Autogrid program (*21*). The AutoDock parameter set- and distance-dependent dielectric functions were used in the calculation of the van der Waals and electrostatic terms, respectively.

Docking simulations were performed using the Lamarckian genetic algorithm (LGA) and the Solis and Wets local search method (*22*). Initial positions, orientations, and torsions of the ligand molecules were set randomly. Each run of the docking experiment was set to terminate after a maximum of 250,000 energy evaluations. The population size was set to 150. During the search, a translational step of 0.2 Å and quaternion and torsion steps of 5 were applied.

RESULTS AND DISCUSSION

Characterization of the Binding Interaction of OTC with BSA by Fluorescence Measurements Based on the Elimination of the Inner Filter Effects. Although there have been some studies on the interaction between OTC and BSA by fluorescence technique (*15*−*18*), the inner filter effect was not considered. In this study, we eliminated the inner filter effect for all of the fluorescence and synchronous fluorescence results to obtain accurate data. To eliminate the inner filter effects of BSA and OTC, absorbance measurements were performed at excitation and emission wavelengths of the fluorescence measurements. The fluorescence intensity was corrected using the equation (*23*)

$$F_{cor} = F_{obs} 10^{(A_1 + A_2)/2} \quad (1)$$

where F_{cor} and F_{obs} are the fluorescence intensity corrected and observed, respectively, and A_1 and A_2 are the sum of the absorbance of BSA and OTC at excitation and emission wavelengths, respectively.

Influence of OTC Concentration on the BSA Fluorescence Intensity. The fluorescence of BSA is quenched by OTC as seen in **Figure 1**. Furthermore, a small blue shift was observed with increasing OTC concentration, which suggests that the fluorescence chromophore of BSA was placed in a more hydrophobic environment after the addition of OTC (*24*).

Quenching mechanisms include static and dynamic quenching (*25*). To confirm the quenching mechanism, the fluorescence quenching data were analyzed according to the Stern−Volmer equation (*26*)

$$\frac{F_0}{F} = 1 + K_{SV}[Q] = 1 + k_q \tau_0 [Q] \quad (2)$$

where F_0 and F are the fluorescence intensities in the absence and presence of the quencher, respectively. K_{SV} is the Stern−Volmer quenching constant, [Q] the concentration of the quencher, k_q the quenching rate constant of the biological macromolecule, and τ_0 the fluorescence lifetime in the absence of quencher.

The Stern−Volmer plots before and after correction are shown in **Figure 2a**. It can be seen that the plot before correction was not linear, so the Stern−Volmer equation cannot be used to calculate K_{SV} and k_q. After correction with eq 1 to remove the inner filter effect, the plot shows results that agree with the Stern−Volmer equation (eq 2). The Stern−Volmer plots for the quenching of BSA by OTC at two different temperatures are shown in **Figure 2b**. The quenching type should be single static or dynamic quenching. Because higher temperature results in larger diffusion coefficients, the dynamic quenching constants will increase with increasing temperature. In contrast, increased temperature is likely to result in decreased stability of complexes, and thus the static quenching constants are expected to decrease with increasing

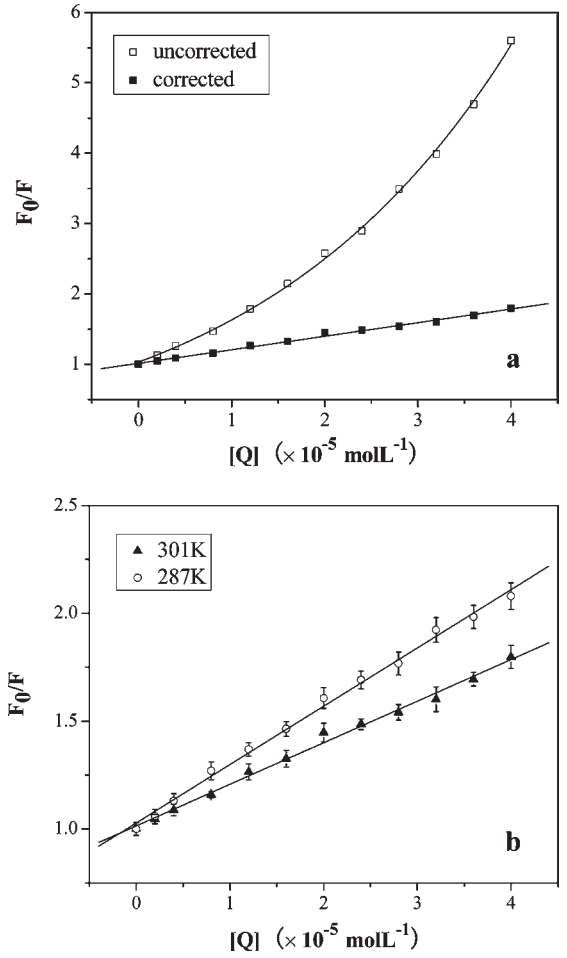

Figure 2. (**a**) Stern−Volmer plots for the quenching of BSA by OTC at 301 K before and after correction; (**b**) Stern−Volmer plots for the quenching of BSA by OTC at different temperatures (corrected). Conditions: BSA, 1.0×10^{-6} mol L^{-1}; pH 7.4.

temperature (*27*). The maximum scatter collision quenching constant of various quenchers with the biopolymer was 2.0×10^{10} L $mol^{-1}s^{-1}$ (*4*). In this paper, K_{SV} and k_q at two different temperatures are listed in the Supporting Information, Supplemental Table 1. The K_{SV} values decreased with increasing temperature, and k_q was $> 2.0 \times 10^{10}$ L mol^{-1} s^{-1}. These results indicate that the quenching was not initiated from dynamic collision but from the formation of a complex.

Association Constants and Number of Binding Sites. For the static quenching interaction, when small molecules bind independently to a set of equivalent sites on a macromolecule, the binding constant (K_a) and the number of binding sites (n) can be determined by the equation (*5*)

$$\lg \frac{(F_0 - F)}{F} = \lg K_a + n \lg [Q] \quad (3)$$

where F_0, F, and [Q] are the same as in eq 2. According to eq 3, values of n and K_a (shown in **Table 1**) at physiological pH 7.4 were calculated. The number of binding sites n approximately equals 1, indicating that there is one binding site in BSA for OTC during their interaction.

Thermodynamic Parameters and Binding Forces. The acting forces between small organic molecules and biomolecules include hydrogen bonds, van der Waals interactions, electrostatic forces, and hydrophobic interaction forces. If the temperature changes little, the reaction enthalpy change ($\Delta H°$) is regarded as a constant. The interaction parameters can be calculated on the basis of the van't Hoff equation

$$\ln\left(\frac{(K_a)_2}{(K_a)_1}\right) = \left(\frac{1}{T_1} - \frac{1}{T_2}\right)\left(\frac{\Delta H°}{R}\right) \quad (4)$$

and thermodynamic equations

$$\Delta G° = \Delta H° - T\Delta S° = -RT \ln K_a \quad (5)$$

where $(K_a)_1$ and $(K_a)_2$ are the binding constants at T_1 and T_2. R is the universal gas constant. $\Delta G°$ and $\Delta S°$ are the free-energy change and the entropy change of the binding reaction, respectively.

If $\Delta H < 0$ and $\Delta S < 0$, van der Waals' interactions and hydrogen bonds play major roles in the binding reaction. If $\Delta H > 0$ and $\Delta S > 0$, hydrophobic interactions are dominant. Electrostatic forces are more important when $\Delta H < 0$ and $\Delta S > 0$ (*27*). The calculated thermodynamic parameters and K_a values for the binding interaction between OTC and BSA are listed in **Table 1**. The negative $\Delta H°$ and positive $\Delta S°$ indicated that electrostatic forces play the major role during the interaction. Because under the experimental conditions used the pH (7.4) is much greater than the isoelectric point of BSA (4.7), BSA is negatively charged. OTC is also negatively charged at pH 7.4 (*28*). Although BSA and OTC^- are both negatively charged, OTC^- can interact with the positively charged amino acid residues of BSA through electrostatic forces (*29*). In addition, the negative sign of $\Delta G°$ indicates the binding of OTC with BSA is spontaneous (*27*).

Table 1. Binding Constants and Relative Thermodynamic Parameters of the OTC−BSA System

T (K)	K_a ($\times 10^4$ L mol^{-1})	n	R^a	$\Delta H°$ (kJ mol^{-1})	$\Delta S°$ (J mol^{-1} K^{-1})	$\Delta G°$ (kJ mol^{-1})
287	1.79	0.96	0.9981	−20.089	11.418	−23.366
301	1.21	0.95	0.99869			−23.526

[a] R is the correlation coefficient for the K_a values.

Energy Transfer between OTC and BSA. According to the Forster's dipole−dipole nonradiative energy transfer theory (*30*), energy transfer from one molecule (donor) to another molecule (acceptor) will happen under the following conditions: (a) the energy donor can produce fluorescence; (b) the absorption spectrum of the receptor sufficiently overlaps with the donor's fluorescence emission spectrum; (c) the distance between the donor and the acceptor is < 8 nm (*31*). The following equation can be used to calculate the efficiency (E) of energy transfer between the donor and acceptor (*32*):

$$E = 1 - \frac{F}{F_0} = \frac{R_0^6}{R_0^6 + r^6} \quad (6)$$

In eq 6, r is the distance between the donor and acceptor and R_0 is the critical distance when the transfer efficiency is 50%, which can be calculated by the equation

$$R_0^6 = 8.79 \times 10^{-25} K^2 n^{-4} \phi J \quad (7)$$

where K^2 is the orientation factor related to the geometry of the donor−acceptor dipole, n is the refractive index of the medium, Φ is the fluorescence quantum yield of the donor, and J expresses the degree of spectral overlap between the donor emission and the acceptor absorption, which can be calculated by the equation (*5*)

$$J = \frac{\int_0^\infty F(\lambda)\varepsilon(\lambda)\lambda^4 \, d\lambda}{\int_0^\infty F(\lambda) \, d\lambda} \quad (8)$$

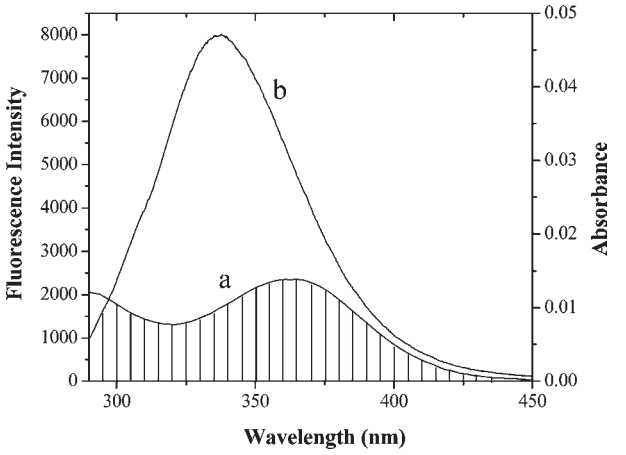

Figure 3. Overlap of the absorption spectra of OTC (a) with fluorescence emission of BSA (b) (corrected). Conditions: c(OTC) = c(BSA) = 1.0 × 10^{-6} mol L^{-1}.

where $F(\lambda)$ is the fluorescence intensity of the donor at wavelength range λ and $\varepsilon(\lambda)$ is the molar absorption coefficient of the acceptor at wavelength λ. Here the donor and acceptor were BSA and OTC, respectively. The overlap of the absorption spectrum of OTC and the fluorescence emission spectrum of BSA is shown in **Figure 3**. J can be evaluated by integrating the spectra in **Figure 3** according to eq 8. For BSA, $K^2 = 2/3$, $n = 1.336$, and $\Phi = 0.15$ (*5*). According to eqs 6−8, the following parameters are obtained: $J = 1.480 \times 10^{-14}$ cm^3 L mol^{-1}, $R_0 = 2.69$ nm, $E = 0.0904$, and $r = 3.95$ nm. The donor (tryptophan residues of the BSA) to acceptor (OTC) distance was < 8 nm, indicating that the energy transfer from BSA to OTC occurred with high probability. However, the most important aspect that should be noted is that the distance calculated here is actually the average value between the bound OTC and the two tryptophan residues in BSA (*33*). The results were in accordance with conditions of Förster theory of nonradioactive energy transfer and indicated again a static quenching between OTC and BSA.

In summary, after elimination of the inner filter effect, we obtain accurate data of the interaction of OTC with BSA including the quenching rate constant, the association constant, the number of binding sites, the thermodynamic parameters, and the average distance between the bound OTC and the two tryptophan residues in BSA, which is different from previous studies (*15*−*18*) (seen in the Supporting Information, Supplemental Table 2).

Identification of the Specific Binding Sites on BSA. Similar to human serum albumin (HSA), the heart-shaped BSA consists of three homologous α-helical domains (I−III). Each domain contains two subdomains (A and B) (seen in the Supporting Information, Supplemental Figure 1). BSA protein model was modeled with CPHmodels. The principal regions of ligand binding sites of albumin are located in hydrophobic cavities in subdomains IIA and IIIA (*34*). Many ligands bind specifically to serum albumin, for example, warfarin and phenylbutazone for site I (subdomain IIA), flufenamic acid (FA) and ibuprofen for site II (subdomain IIIA), and digitoxin for site III (*35*). **Table 2** shows the changes in fluorescence of OTC bound to BSA on the addition of other drugs. OTC was not significantly displaced by phenylbutazone or by digitoxin. However, flufenamic acid (subdomain IIIA) gave a significant displacement of OTC, suggesting that OTC's binding site on BSA is subdomain IIIA. OTC^- can bind with the positively charged amino acid residues of the subdomain IIIA of BSA through electrostatic forces.

To further define the binding site, considering the nearby positively charged amino acid residues (Arg, Lys, and His) as a group (**Figure 4**), we divide the positively charged amino acid residues of the subdomain IIIA of BSA into eight groups (1−8) (**Table 3**). The surface area (*36*) and the evolutionary conservation (*37*,*38*) of the group residues, the distance between the group residues and Trp in BSA, were investigated. For the evolutionary conservation evaluation, nine grades were assigned. A higher grade indicates higher conservation of the residues, which increases the likelihood of the region as the binding site (*39*). The ideal positively charged amino acid residues that bind with OTC^- should satisfy with the following conditions: (1) sufficient surface area (*40*); (2) the distance between residues and the two Trp residues of BSA should include the calculated 3.95 nm; (3) high evolutionary conservation scores. According to the conditions, the excluded items are marked with bold italic in **Table 3**. It can be seen from **Table 3** that the most likely binding sites are group 1, followed by group 2, and then group 3.

Table 2. Effects of Site Probe on the Binding Constant of OTC to BSA

K (without the site probe) (10^4 L mol^{-1})	K (with PB) (10^4 L mol^{-1})	K (with FA) (10^4 L mol^{-1})	K (with Dig) (10^4 L mol^{-1})
1.21	1.20	0.27	1.14

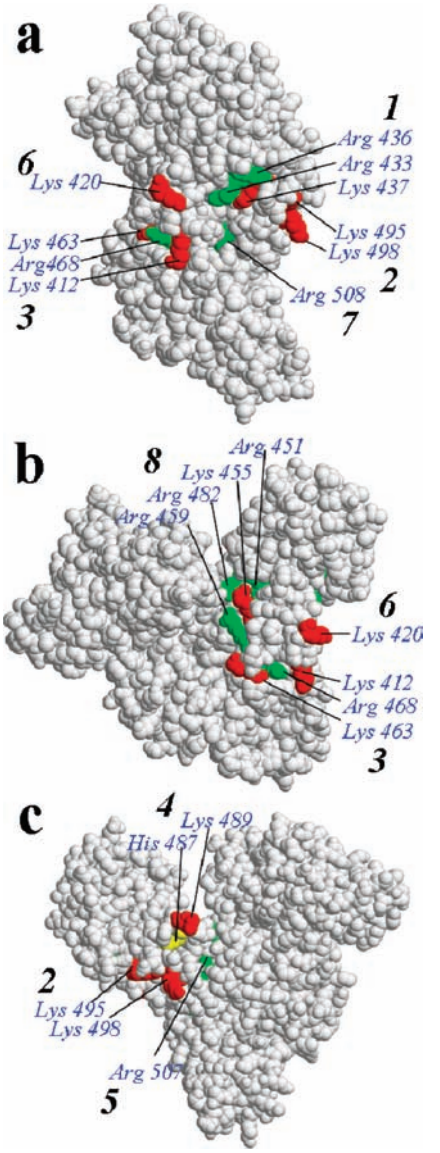

Figure 4. Positive charged amino acid residues (Arg, Lys, and His) of the subdomain IIIA of BSA viewed from different perspectives.

Table 3. Accessible Surface Area, Distance between Residues and Trp of BSA, Evolutionary Conservation Scores of the Positive Charged Residues of Subdomain IIIA of BSA, and Estimated Free Energy of OTC Binding with Possible Binding Sites

possible binding sites	positive charged residues of subdomain IIIA	accessible surface area (Å^2)	distance between residues and Trp of BSA (Å)		evolutionary conservation scores of residues	estimated free energy of binding (kcal/mol)
			Trp-237	Trp-158		
1	Arg 433	78.15	30.86	42.33	grade 6	−3.33
	Arg 436	54.95	32.68	45.01	grade 5	
	Lys 437	29.79	30.88	44.06	grade 7	
2	Lys 495	68.95	25.31	43.74	***grade 2***	−2.82
	Lys 498	132.59	21.55	42.77	grade 7	
3	Lys 412	90.97	24.98	42.77	grade 8	−2.91
	Lys 463	73.38	23.17	34.28	grade 0	
	Arg 468	45.39	18.55	35.54	grade 4	
4	His 487	***16.87***	***24.92***	***34.28***	grade 6	−2.47
	Lys 489	193.89	***27.96***	***35.8***	***grade 3***	
5	Arg 507	***12.60***	14.47	38.11	grade 9	−1.90
6	Lys 420	171.24	35.04	42.46	***grade 2***	−2.03
7	Arg 508	27.40	***15.38***	***37.95***	grade8	188.08
8	Arg 451	21.87	***28.28***	***30.51***	***grade 2***	6.15
	Lys 455	51.57	***25.51***	***28.84***	***grade 3***	
	Arg 459	80.19	***23.07***	***29.43***	***grade 3***	
	Arg 482	65.88	***18.95***	***27.75***	grade 5	

To confirm the results obtained above, molecule docking was employed by setting the simulation box to the different likely binding sites (groups 1−8). The energy-ranked results of each site are shown in **Table 3**. Group 1 has the lowest free energy of binding, confirming the result that OTC$^-$ interacts with group 1. As shown in **Figure 5**, there is electrostatic interaction between Arg 433 and the oxygen atoms at positions 19 and 22. The electrostatic interaction also exists between Arg 436 and the oxygen atoms at positions 20 and 23. The carbon atoms at positions 2, 16, and 17 have hydrophobic interactions with Ala 429, Pro 516, and Pro 516, respectively. Hydrogen bonding and other forces also exist, but the electrostatic forces play a major role in the binding of OTC$^-$ to BSA.

Investigation of BSA Conformation Changes. To explore the effect of OTC on the conformation changes of BSA, UV−vis absorption spectra, CD, and synchronous fluorescence measurements were performed.

UV−Vis Absorption Spectra Studies. UV−vis absorption spectroscopy technique can be used to explore the structural changes of protein and to investigate protein−ligand complex formation. The UV−vis absorption spectra of BSA in the presence and absence of OTC are shown in **Figure 6**. BSA has two absorption peaks. The strong absorption peak at about 208 nm reflects the framework conformation of the protein (*41*). The weak absorption peak at about 279 nm appears to be due to the aromatic amino acids (Trp, Tyr, and Phe) (*42*). With gradual addition of OTC to BSA solution, the intensity of the peak at 208 nm decreases and red shifts and the intensity of the peak at 279 nm also decreases. The results indicate that the interaction between OTC and BSA leads to the loosening and unfolding of the protein skeleton and increases the hydrophobicity of the microenvironment of the aromatic amino acid residues (*43*).

Synchronous Fluorescence. Synchronous fluorescence spectroscopy can give information about the molecular environment in the vicinity of chromophores. The spectrum is obtained through the simultaneous scanning of the excitation and emission

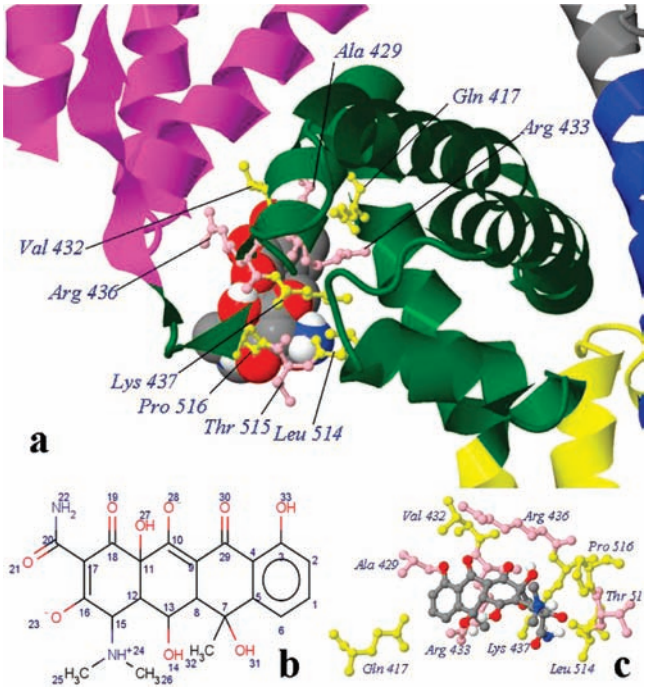

Figure 5. (**a**) Binding mode between OTC$^-$ and BSA; (**b**) 2D structure of OTC$^-$ with atom numbers; (**c**) binding mode between OTC$^-$ and the interacting residues of BSA. The atoms of OTC$^-$ are color-coded as follows: O, red; N, blue; C, gray; H, white. The subdomains of BSA are color-coded as follows: green, IIIA; magenta, IIIB; blue, IIA; yellow, IIB; gray, IB.

monochromators while maintaining a constant wavelength interval between them. When the wavelength intervals ($\Delta\lambda$) are stabilized at 15 or 60 nm, synchronous fluorescence gives the characteristic information of tyrosine residues or tryptophan residues, respectively (*44*).

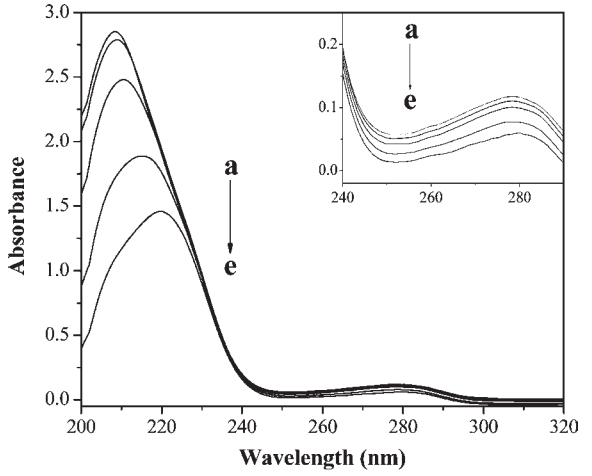

Figure 6. UV−vis spectra of BSA in the presence of different concentrations of OTC (vs the same concentration of OTC solution). Conditions: BSA, 2.5×10^{-6} mol L^{-1}; OTC/(10^{-5} mol L^{-1}), a, 0; b, 2; c, 8; d, 15; e, 20; pH 7.4; T = 301 K.

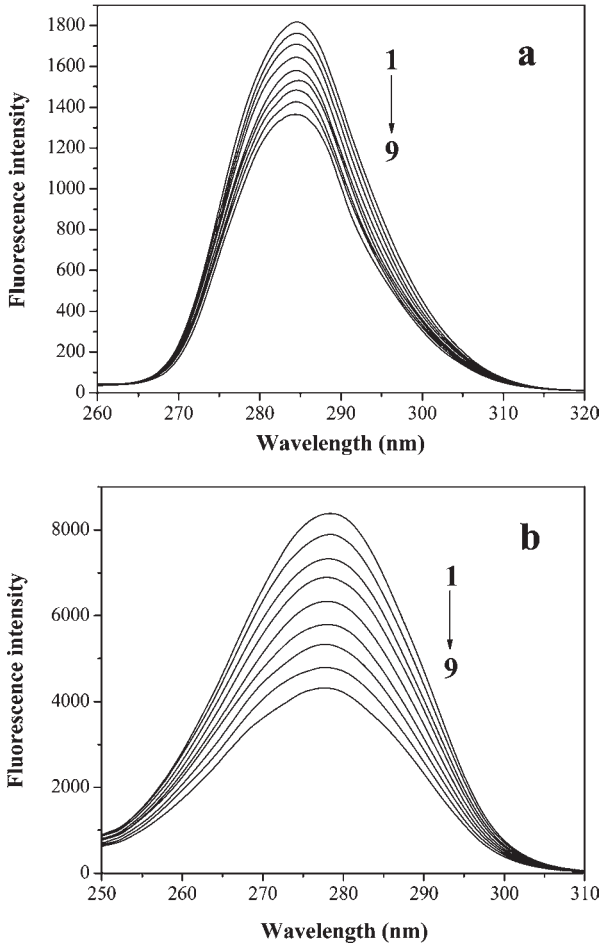

Figure 7. Synchronous fluorescence spectra of BSA (corrected): (**a**) $\Delta\lambda$ = 15 nm; (**b**) $\Delta\lambda$ = 60 nm. Conditions: BSA, 1.0×10^{-6} mol L^{-1}; OTC/(10^{-5} mol L^{-1}), 1, 0; 2, 0.5; 3, 1; 4, 1.5; 5, 2; 6, 2.5; 7, 3; 8, 3.5; 9, 4; T = 301 K.

The synchronous fluorescence spectra of BSA with various amounts of OTC in **Figure 7a** show that the emission peaks do not shift over the investigated concentration range, which indicates that OTC has little effect on the microenvironment of the tyrosine residues in BSA. In **Figure 7b**, the emission maximum of tryptophan

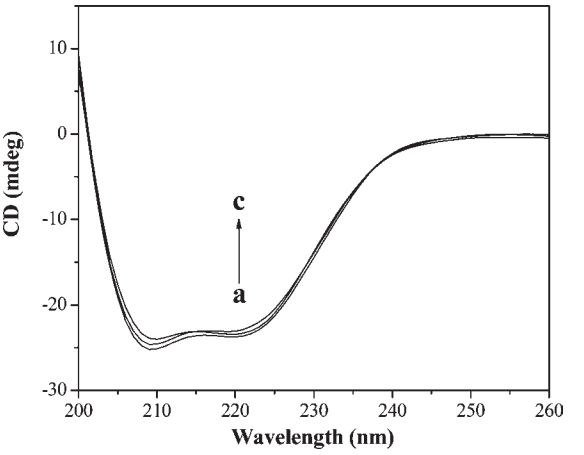

Figure 8. CD spectra of BSA and BSA−OTC system. Conditions: BSA, 2.0×10^{-7} mol L^{-1}; molar ratios of OTC to BSA, a, 0:1; b, 1:1; c, 2.5:1; pH 7.4; T = 301 K.

residues shows a slight blue shift (from 278.6 to 277.6 nm), which indicates that the conformation of BSA was changed such that the polarity around the tryptophan residues decreased and the hydrophobicity was increased (*45*).

Circular Dichroism. To ascertain the possible influence of OTC binding on the secondary structure of BSA, CD measurements were performed in the presence of different OTC concentrations (**Figure 8**). The CD spectra of BSA exhibited two negative bands in the ultraviolet region at about 208 and 222 nm, which is characteristic of the α-helix of proteins (*46*). The α-helical contents of BSA in the absence and presence of OTC were calculated from eqs 9 and 10:

$$\text{MRE} = \frac{\text{observed CD (mdeg)}}{C_P n l \times 10} \tag{9}$$

In eq 9 C_P is the molar concentration of the protein, n is the number of amino acid residues (574), and l is the path length of the cell (1 cm).

$$\alpha\text{-helix (\%)} = \frac{-\text{MRE}_{208} - 4000}{33000 - 4000} \times 100 \tag{10}$$

In eq 10 MRE_{208} is the observed MRE value at 208 nm, 4000 is the MRE where the β-form and random coil conformation cross at 208 nm, and 33000 is the MRE value of a pure α-helix at 208 nm. With the addition of OTC to BSA (1:1 and 2.5:1), the α-helicity decreased from 59.56% in free BSA to 57.76 and 55.27%, respectively. The decrease of α-helix content indicates that the binding of OTC with BSA induces some conformational changes in BSA (*5*), which may affect the physiological functions of BSA.

As mentioned above, the binding of OTC can lead to the loosening and unfolding of the protein skeleton and increases the hydrophobicity of the microenvironment of the tryptophan residues of BSA. The α-helix of the secondary structure of BSA decreased due to the binding of OTC.

ABBREVIATIONS USED

OTC, oxytetracycline; BSA, bovine serum albumin; PB, phenylbutazone; FA, flufenamic acid; CD, circular dichroism.

ACKNOWLEDGMENT

We thank Dr. Pamela Holt for editing the manuscript for English.

Supporting Information Available: Domain structure of bovine serum albumin, Stern−Volmer quenching constants, and comparison of the binding parameters of our results after the elimination of the inner filter effect with previous studies. This material is available free of charge via the Internet at http://pubs.acs.org.

LITERATURE CITED

(1) Huang, B. X.; Kim, H. Y.; Dass, C. Probing three-dimensional structure of bovine serum albumin by chemical cross-linking and mass spectrometry. *J. Am. Soc. Mass Spectrom.* **2004**, *15*, 1237–1247.

(2) Tian, J.; Liu, J.; Hu, Z.; Chen, X. Interaction of wogonin with bovine serum albumin. *Bioorg. Med. Chem.* **2005**, *13*, 4124–4129.

(3) Xiang, G.; Tong, C.; Lin, H. Nitroaniline isomers interaction with bovine serum albumin and toxicological implications. *J. Fluoresc.* **2007**, *17*, 512–521.

(4) Zhang, Y. Z.; Zhou, B.; Zhang, X. P.; Huang, P.; Li, C. H.; Liu, Y. Interaction of malachite green with bovine serum albumin: determination of the binding mechanism and binding site by spectroscopic methods. *J. Hazard. Mater.* **2009**, *163*, 1345–1352.

(5) Wang, N.; Ye, L.; Yan, F. F.; Xu, R. Spectroscopic studies on the interaction of azelnidipine with bovine serum albumin. *Int. J. Pharm.* **2008**, *351*, 55–60.

(6) Brillantes, S.; Tanasomwang, V.; Thongrod, S.; Dachanantawitaya, N. Oxytetracycline residues in giant freshwater prawn (*Macrobrachium rosenbergii*). *J. Agric. Food Chem.* **2001**, *49*, 4995–4999.

(7) Kurittu, J.; Lonnberg, S.; Virta, M.; Karp, M. A group-specific microbiological test for the detection of tetracycline residues in raw milk. *J. Agric. Food Chem.* **2000**, *48*, 3372–3377.

(8) Moats, W. A. Determination of tetracycline antibiotics in beef and pork tissues using ion-paired liquid chromatography. *J. Agric. Food Chem.* **2000**, *48*, 2244–2248.

(9) Pena, A.; Lino, C. M.; Alonso, R.; Barcelo, D. Determination of tetracycline antibiotic residues in edible swine tissues by liquid chromatography with spectrofluorometric detection and confirmation by mass spectrometry. *J. Agric. Food Chem.* **2007**, *55*, 4973–4979.

(10) Rigos, G.; Nengas, I.; Alexis, M.; Troisi, G. M. Potential drug (oxytetracycline and oxolinic acid) pollution from Mediterranean sparid fish farms. *Aquat. Toxicol.* **2004**, *69*, 281–288.

(11) Kong, W. D.; Zhu, Y. G.; Liang, Y. C.; Zhang, J.; Smith, F. A.; Yang, M. Uptake of oxytetracycline and its phytotoxicity to alfalfa (*Medicago sativa* L.). *Environ. Pollut.* **2007**, *147*, 187–193.

(12) De Jonge, H. R. Toxicity of tetracyclines in rat-small-intestinal epithelium and liver. *Biochem. Pharmacol.* **1973**, *22*, 2659–2677.

(13) Wang, W.; Lin, H.; Xue, C.; Khalid, J. Elimination of chloramphenicol, sulphamethoxazole and oxytetracycline in shrimp, *Penaeus chinensis* following medicated-feed treatment. *Environ. Int.* **2004**, *30*, 367–373.

(14) Qu, M. M.; Sun, L. W.; Chen, J.; Li, Y. Q.; Chen, Y. G.; Kong, Z. M. Toxicological characters of arsanilic acid and oxytetracycline. *J. Agro-Environ. Sci.* **2004**, *23*, 240–242.

(15) Khan, M. A.; Muzammil, S.; Musarrat, J. Differential binding of tetracyclines with serum albumin and induced structural alterations in drug-bound protein. *Int. J. Biol. Macromol.* **2002**, *30*, 243–249.

(16) Ma, J. K.; Jun, H. W.; Luzzi, L. A. Tetracycline binding to bovine serum albumin studied by fluorescent techniques. *J. Pharm. Sci.* **1973**, *62*, 1261–1264.

(17) Popov, P. G.; Vaptzarova, K. I.; Kossekova, G. P.; Nikolov, T. K. Fluorometric study of tetracycline−bovine serum albumin interaction. The tetracyclines − a new class of fluorescent probes. *Biochem. Pharmacol.* **1972**, *21*, 2363–2372.

(18) Bi, S.; Song, D.; Tian, Y.; Zhou, X.; Liu, Z.; Zhang, H. Molecular spectroscopic study on the interaction of tetracyclines with serum albumins. *Spectrochim. Acta A: Mol. Biomol. Spectrosc.* **2005**, *61*, 629–636.

(19) Halgren, T. A. Merck molecular force field. I. Basis, form, scope, parametrization, and performance of MMFF94. *J. Comput. Chem.* **1998**, *17*, 490–519.

(20) Lund, O.; Nielsen, M.; Lundegaard, C.; Worning, P. CPHmodels 2.0: X3M a computer program to extract 3D models. *Abstracts from the CASP5 Conference* **2002**, *A102*; http://www.cbs.dtu.dk/services/CPHmodels.

(21) Morris, G. M.; Halliday, R. S.; Huey, R.; Hart, W. E.; Belew, R. K.; Olson, A. J.; Goodsell, D. S. Automated docking using a Lamarckian genetic algorithm and an empirical binding free energy function. *J. Comput. Chem.* **1998**, *19*, 1639–1662.

(22) Solis, F. J.; Wets, R. J. B. Minimization by random search techniques. *Math. Operations Res.* **1981**, *6*, 19–30.

(23) Shyamali, S. S.; Lillian, D. R.; Lawrence, L.; Esther, B. Fluorescence studies of native and modified neurophysins. Effects of peptides and pH. *Biochemistry* **1979**, *18*, 1026–1036.

(24) Yuan, T.; Weljie, A. M.; Vogel, H. J. Tryptophan fluorescence quenching by methionine and selenomethionine residues of calmodulin: orientation of peptide and protein binding. *Biochemistry* **1998**, *37*, 3187–3195.

(25) Papadopoulou, A.; Green, R. J.; Frazier, R. A. Interaction of flavonoids with bovine serum albumin: a fluorescence quenching study. *J. Agric. Food Chem.* **2005**, *53*, 158–163.

(26) Soares, S.; Mateus, N.; Freitas, V. Interaction of different polyphenols with bovine serum albumin (BSA) and human salivary α-amylase (HSA) by fluorescence quenching. *J. Agric. Food Chem.* **2007**, *55*, 6726–6735.

(27) Khan, S. N.; Islam, B.; Yennamalli, R.; Sultan, A.; Subbarao, N.; Khan, A. U. Interaction of mitoxantrone with human serum albumin: spectroscopic and molecular modeling studies. *Eur. J. Pharm. Sci.* **2008**, *35*, 371–382.

(28) Jiao, S.; Zheng, S.; Yin, D.; Wang, L.; Chen, L. Aqueous oxytetracycline degradation and the toxicity change of degradation compounds in photoirradiation process. *J. Environ. Sci.* (*China*) **2008**, *20*, 806–813.

(29) Pan, X. R.; Liu, R. T.; Qin, P. F.; Wang, L.; Zhao, X. C. Spectroscopic studies on the interaction of acid yellow with bovine serum albumin. *J. Lumin.* **2010**, *130*, 611–617.

(30) Förster, T. Delocalized excitation and excitation transfer. In *Modern Quantum Chemistry*; Academic Press: New York, 1996; pp 93−137.

(31) Valeur, B.; Brochon, J. C. *New Trends in Fluorescence Spectroscopy*; Springer Press: Berlin, Germany, 2001; p 25.

(32) Horrocks, W. D., Jr.; Snyder, A. P. Measurement of distance between fluorescent amino acid residues and metal ion binding sites. Quantitation of energy transfer between tryptophan and terbium(III) or europium(III) in thermolysin. *Biochem. Biophys. Res. Commun.* **1981**, *100*, 111–117.

(33) Liu, J.; Tian, J. N.; Zhang, J.; Hu, Z.; Chen, X. Interaction of magnolol with bovine serum albumin: a fluorescence-quenching study. *Anal. Bioanal. Chem.* **2003**, *376*, 864–867.

(34) Zhou, N.; Liang, Y. Z.; Wang, P. 18β-Glycyrrhetinic acid interaction with bovine serum albumin. *J. Photochem. Photobiol. A−Chem.* **2007**, *185*, 271–276.

(35) Bian, H. D.; Li, M.; Yu, Q.; Chen, Z. F.; Tian, J. N.; Liang, H. Study of the interaction of artemisinin with bovine serum albumin. *Int. J. Biol. Macromol.* **2006**, *39*, 291–297.

(36) Tsodikov, O. V.; Record, M. T.; Sergeev, Y. V. Novel computer program for fast exact calculation of accessible and molecular surface areas and average surface curvature. *J. Comput. Chem.* **2002**, *23*, 600–609.

(37) Landau, M.; Mayrose, I.; Rosenberg, Y.; Glaser, F.; Martz, E.; Pupko, T.; Ben-Tal, N. ConSurf 2005: the projection of evolutionary conservation scores of residues on protein structures. *Nucleic Acids Res.* **2005**, *33*, W299–W302.

(38) Glaser, F.; Pupko, T.; Paz, I.; Bell, R. E.; Bechor-Shental, D.; Martz, E.; Ben-Tal, N. ConSurf: identification of functional regions in proteins by surface-mapping of phylogenetic information. *Bioinformatics* **2003**, *19*, 163–164.

(39) Martz, E. Protein Explorer: easy yet powerful macromolecular visualization. *Trends Biochem. Sci.* **2002**, *27*, 107–109.

(40) Cai, W. S.; Shao, X. G.; Maigret, B. Protein-ligand recognition using spherical harmonic molecular surfaces: towards a fast and efficient filter for large virtual throughput screening. *J. Mol. Graphics Modell.* **2002**, *20*, 313–328.

(41) Yang, Q.; Liang, J.; Han, H. Probing the interaction of magnetic iron oxide nanoparticles with bovine serum albumin by spectroscopic techniques. *J. Phys. Chem. B* **2009**, *113*, 10454–10458.

(42) Wang, F.; Huang, W.; Dai, Z. X. Spectroscopic investigation of the interaction between riboflavin and bovine serum albumin. *J. Mol. Struct*. **2008**, *875*, 509–514.
(43) Wu, T.; Wu, Q.; Guan, S.; Su, H.; Cai, Z. Binding of the environmental pollutant naphthol to bovine serum albumin. *Biomacromolecules* **2007**, *8*, 1899–906.
(44) Wang, Y. Q.; Zhang, H. M.; Zhang, G. C.; Liu, S. X.; Zhou, Q. H.; Fei, Z. H.; Liu, Z. T. Studies of the interaction between paraquat and bovine hemoglobin. *Int. J. Biol. Macromol*. **2007**, *41*, 243–250.
(45) Hu, Y. J.; Liu, Y.; Pi, Z. B.; Qu, S. S. Interaction of cromolyn sodium with human serum albumin: a fluorescence quenching study. *Bioorg. Med. Chem*. **2005**, *13*, 6609–14.
(46) Lu, J. Q.; Jin, F.; Sun, T. Q.; Zhou, X. W. Multi-spectroscopic study on interaction of bovine serum albumin with lomefloxacin−copper(II) complex. *Int. J. Biol. Macromol*. **2007**, *40*, 299–304.

Received for review April 15, 2010. Revised manuscript received August 16, 2010. Accepted August 17, 2010. The work is supported by NSFC (20875055), the Cultivation Fund of the Key Scientific and Technical Innovation Project, Ministry of Education of China (708058), and Excellent Young Scientists and Key Science−Technology Project in Shandong Province (2007BS08005, 2008GG10006012).